

fMRI and MEG Representational Similarity based Fusion

Haider Al-Tahan
Computer Science
Email: haltaha@uwo.ca

Nicky Bayat
Computer Science
Email: nbayat5@uwo.ca

Abstract—Brain neuronal activations can be represented as complex spatio-temporal measurements. Current non-invasive neuro-imaging methods (Magnetoencephalography, MEG; Functional magnetic resonance imaging, fMRI) are capable of capturing high resolution spatial or temporal component but not both. Recent work proposed an integration approach that uses representational similarities analysis [1] to combine measurements of MEG and fMRI to yield a rich spatio-temporal representation of brain neuronal activations [2]. Although this method has been shown reliable [3], there is little understanding on the effect of utilizing different similarity metrics when computing this approach. In this project, we aim to investigate the reliability of this method across different similarity metrics by comparing metric results within subjects across visual stimuli of similar conditions. Our results suggests that the choice of distance metric to compute the RDM does not effect the reproducibility of the RDMs when dealing with fMRI data. Alternatively, with MEG data, Mahalanobis distance showed the most reliable results relative to Euclidean and Pearson distances. Lastly, with fMRI/MEG fused data, we found Mahalanobis distance is the most reliable metric to relate the RDMs IT resulting in the significantly highest correlation across twin sets.

Magnetoencephalography, spatio-temporal, functional magnetic resonance imaging, representational similarities analysis.

I. INTRODUCTION

Neurons in the human brain are the basic building block of the nervous system. It is estimated that the human brain consist of billions of neurons with their subsequent connections. Allowing us to accomplish extraordinary behavioural tasks (e.g. writing a research paper). Neuroscientists aims to capture and understand the neural underpinning of various systems (e.g. visual, auditory systems) that aid us in accomplishing those tasks. However, capturing and interpreting individual neuronal activations

are difficult, especially when dealing with that magnitude of information. Instead, neuroscientists measure high representational information about neuronal populations, giving them an intuition over the flow of information within and between populations under controlled behavioural tasks (e.g. looking at an image or hearing music) over many trials.

Many of our basic behaviors rely on multitude of distributed brain networks, a key objective in neuroscience remains to locate brain neuronal activations to build maps of how the brain is organized. One of the most common non-invasive methods that help us investigate the flow of activations in the brain is functional magnetic resonance imaging (fMRI). FMRI uses strong magnetic fields to measure blood flow in the brain and create 3-dimensional brain images consisting of sampling units known as voxel (Figure 1B). These voxels are imbedded with the hemodynamic responses of specific regions in the brain [4], [5]. Hemodynamic responses are the processes that increase blood flow to active neuronal tissues in the brain. Although, neural activities are fast - occurring in matter of milliseconds - hemodynamic responses are slow. The increase in blood flow after a neuronal activation takes a magnitude of seconds to be observable. Nonetheless, fMRI allows us to acquire 3-dimensional brain images that capture changes in hemodynamic response location in the brain within millimeters of precision, this rich data provides a high spatial resolution of the brain activity [4], [5].

One limitation of high spatial resolution in fMRI is that it limits our sampling rate (temporal resolution), that is the number of brain images per fixed time point. Moreover, the fMRI measurements do not directly reflect neuronal

activations. To remedy these limitations in fMRI, neuroscientists use a different method known as magnetoencephalography (MEG). MEG allows us to directly measure neural activations in the time frame in which cognition occurs (high temporal resolution; Figure 1A). When electrically charged ions pass through neurons in the brain, they generate electromagnetic fields [6]. MEG uses SQUID (superconducting quantum interference device) sensors to measure and amplify those electromagnetic fields generated by a population of neurons. Although MEG has high temporal precision, its spatial resolution, is relatively low compared to fMRI. The spatial resolution of MEG is determined by the number of sensors, it is common for MEG devices to have up to 306 sensors. Lastly, unlike fMRI, MEG has relatively less accurate measurements of neuronal activations that reside deeper or below the surface of the brain.

A fundamental challenge in computational neuroscience is using these rich spatio-temporal measurements to study how the brain operates, and to compare these measurements with computational models (e.g. Neural Networks) which are represented in different measurements. Relatively recent approach that allow us to compare and investigate different type of data (e.g. behavioural, neuronal, computational, etc...) is representational similarity analysis (RSA [1], [7], [8]). RSA takes advantage of the predefined stimulus categories to create dissimilarity representations by comparing activity patterns for similar and dissimilar stimuli, resulting in a representational dissimilarity matrix (RDM). Each cell in an RDM represent the dissimilarity between the activity pattern of two experimental stimuli, with a diagonal being zeros as they are the most similar (Figure 1C). The dissimilarities can be computed using any distance metric (e.g. Euclidean distance, Cosine distance, etc...). However, [2], [9] have shown that the reliability of RSA can vary across data types and distance metrics used to compute those RDMs.

Recent work with the goal of capturing rich spatio-temporal resolution brain data, combined both MEG and fMRI using RSA [10]. [10] combined MEG and fMRI by computing MEG RDMs at each time point using SVM decoding accuracy as dissimilarity metric and fMRI RDM

at each voxel using Pearson's correlation as dissimilarity metric. At each time point t , MEG RDM R_t^m was compared using Spearman's correlation r_s with fMRI RDMs R_v^f at each voxel v . Giving us, the degree of similarity between MEG and fMRI RDMs at specific time and voxel $\phi(t, v)$.

$$\forall t \in T, v \in V: \phi(t, v) = r_s(R_t^m, R_v^f) \quad (1)$$

where $T = 1 \dots 1200$ (number of seconds in MEG trial) and $V =$ all the brain voxels in fMRI (Eq. 1). This approach is based on 2 principles, (i) if 2 neuronal representations are similarly represented in fMRI, they should also be similarly represented in MEG and (ii) neuronal representations reflect activations of specific brain region. Hence, higher degree of similarity between MEG and fMRI RDMs means higher level of brain activation at specific time and space.

Although similarity based fusion has been used in numerous studies [3], [11], [12], little is known about the reliability of using different dissimilarity metrics when computing the RDMs. In this project, we investigate the relative contribution of using different dissimilarity metrics when computing MEG and fMRI similarity based fusion. We compare fusion results of the two image sets (twin set images) that were presented to participants during the MEG and fMRI experiments. These image sets have different appearances but share the same semantic information (Twin sets, 2). Similarity based fusion will be computed using Euclidean distance, Pearson correlation, and Mahalanobis distances. The underlying assumption is that if two representations are similarly represented in one dissimilarity metric, then they should also be similarly represented on the same dissimilarity metric on different stimuli of the same semantics but different appearance. Hence, to assess the performance of each metric in constructing RDMs, we compare RDMs for fMRI and MEG on twin set 1 and twin set 2 stimuli. The metric that shows the non-significant variation would be the most suitable for similarity based fusion with fMRI and MEG.

II. DATA

In this project, we utilize MEG and fMRI data acquired from [3]. The dataset consist of two

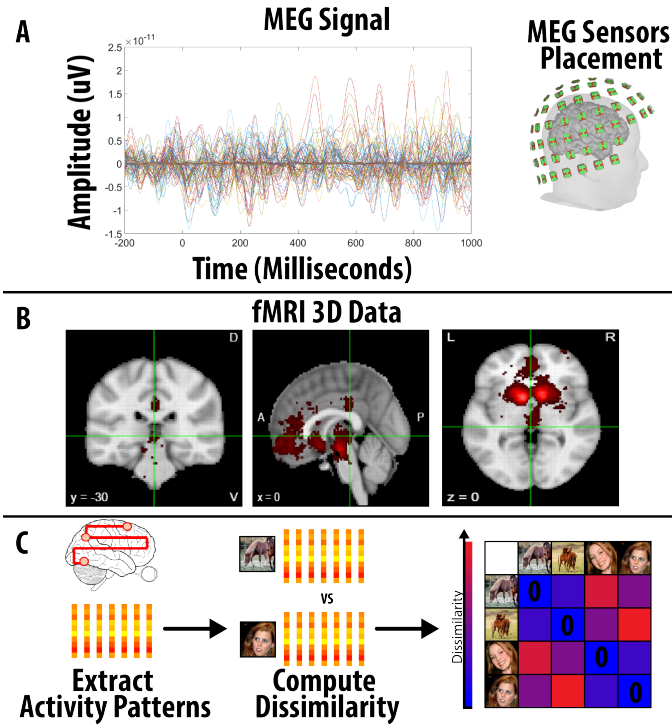


Fig. 1. Data Representations. A) MEG signals of 306 sensors across 1200 time points (1 trial) measured in micro volts. Each sensor is placed in the predefined location on the brain as can be seen on the right. B) Visualization of the 3-dimensional fMRI data at $x = 0, y = -30, z = 0$. C. Example of an representational dissimilarity matrix (RDM) of four different experimental stimuli (2 of which from different categories). RMDs are symmetrical matrices with diagonal being zeros, higher values at each cell indicate higher differences between two pair of activity patterns

independent experiments for different measurements - one for MEG and the other for fMRI - that required participants to look at images from five different categories. During both experiments, images were overlaid with a black fixation cross at the center of the screen for 500 ms. Participants were instructed to respond as quickly as possible to targets by pressing a button and eye blinking upon detection of a specific image. Images were presented once per run in random order. The dataset consist of fifteen right-handed participants with normal or corrected to normal vision. Participants performed the same experiment in fMRI or MEG scanners in separate sessions. There are two image sets that consist of 78 real world natural images each (156 images in total) acquired from the LaMem dataset [13](Figure 2). Each image set contains the same semantic content but different in appearances, hence, they are referred



Fig. 2. Twinset Examples. Examples of the stimuli used in both experiments (fMRI and MEG). The stimuli consist of two sets with different appearance but the same semantic content. Each of the twin set consist 78 images equally distributed across five categories.

as twin set. [3] have also shown that both twinsets were not significantly different on a collection of low level image statistics. Lastly, the data were collected over one MEG session and two fMRI sessions.

The fMRI data consist of 3D matrix representing the whole brain with a of size $53 \times 63 \times 52$ for each trial/stimuli (156 total). In this project, we focus on two major brain areas (or voxels) that are found to play essential roles in human's visual system: (i) Calcarine, is where the central and peripheral visual fields are located. (ii) Inferior temporal gyrus (IT), which is associated with object recognition [14]. Alternatively, the MEG data consist of 306 channels/sensors with 1200 milliseconds of recording for each trial, resulting in a 306×1200 matrix for each trial.

III. METHODS

In this section, we will describe the process of creating the fMRI and MEG RDMs, further, we describe the metrics used to compute the RDMs and the process of computing similarity based fusion. All fMRI and MEG RDMs are 2D matrices of size 156×156 , with 156 being the number of stimuli/images that were presented to the participants for both twin sets combined. The RDMs are based on dissimilarity between pairs of activity patterns (fMRI or MEG) of different stimuli. An RDM that shows perfect dissimilarity within all categories would have near zero dissimilarity for all activity patterns that share similar categorical stimuli (Figure 3). To assess the performance of each dissimilarity metric in constructing RDMs, we compare RDMs for fMRI and MEG on twin set 1 and 2 stimuli. The metric that shows the no-significant variation would be the most suitable for similarity based fusion of fMRI and MEG.

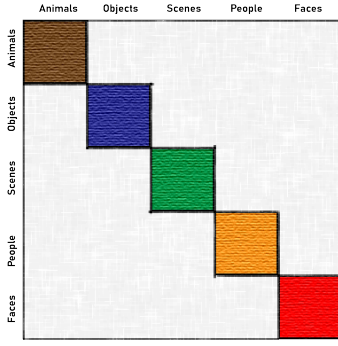


Fig. 3. Perfect RDM. An RDM that shows perfect dissimilarity within all categories, having near zero dissimilarity for all activity patterns that share similar categorical stimuli. Thereby, creating cubic shapes around the diagonal axis of an RDM

A. RDM Metrics

In order to compute the RDMs, we need a function $d(x, y)$ that gives us a measurement of how dissimilar two elements are. Elements in this context can be any arbitrary objects (e.g. vectors, scalars). In this project, we focus on three major distance metrics.

$$d(x, y) = 1 - \frac{\sum_{i=1}^n (x_i - \bar{x})(y_i - \bar{y})}{\sqrt{\sum_{i=1}^n (x_i - \bar{x})^2(y_i - \bar{y})^2}} \quad (2)$$

The first metric (Eq. 2) utilizes the Pearson correlation coefficient to measure the linear relationships between two elements. However, Pearson correlation coefficients have a range of $[-1, 1]$, with higher value indicating more similar elements. We compute the dissimilarity using Pearson correlation coefficient by subtracting 1 by Pearson correlation coefficient (1-corr), resulting in dissimilarity range of $[0, 2]$. This metric will be referred to as 'correlation' distance metric throughout the text, instead of, '1 - correlation'.

$$d(x, y) = \sqrt{\sum_{i=1}^n (x_i - y_i)^2} \quad (3)$$

The second metric (Eq. 3) is the Euclidean distance, in a 2d plane the Euclidean distance measures the straight line between two points. The Euclidean distance measures the square root of the sum of squared element-wise differences between

two vectors. Hence, the higher the values are the more dissimilar the vectors are, with ranges being always positive i.e. $[0, \infty)$.

$$d(x, y) = \sqrt{(x - y)^T Cov^{-1}(x - y)} \quad (4)$$

One limitation of the Euclidean distance is that it does not account for the differences in variance between two elements from the same distribution . To overcome this limitation we utilize the Mahalanobis distance (Eq. 4) by incorporating the covariance matrix in our calculations. The covariance matrix is a symmetrical matrix where the diagonal elements are variances of the distribution of the elements and the symmetrical elements are the covariances. It is worth noting that if the covariance matrix is the identity matrix then Mahalanobis distance is just the Euclidean distance.

B. fMRI and MEG RDM Construction

In order to compute RDMs, we need to extract a vectorized version of our multidimensional activity patterns for each condition, then compute the dissimilarity across all vectorized activity patterns. Hence, each cell in an RDM represent the dissimilarity between the activity pattern of two experimental stimuli, with a diagonal being zeros as the same elements are the most similar.

For fMRI, we compute the RDMs for two brain areas (i.e. IT and Calcarine). Given a matrix of size $[53, 63, 52]$ we apply pre-defined masks of the same size as the data that capture the area for each region of interest. After extracting the activity patterns of the region of interest, we squeeze the 3D matrix to a 1D vector, resulting in a vector with varying size that is dependent on the total area of the voxel. We perform this computation for every trial and region. This result in V matrices of size $[N, N]$, where V is the number of voxels and N is the number of stimuli (Figure 4). Alternatively, for MEG we have a time-series matrices of size $[306, 1200]$ for each trial, we extract a vector of size $S = 306$ for all the sensors at each time point $T = 1200$. This result in T matrices of size $[N, N]$ (Figure 4).

C. fMRI and MEG Fusion

In order to compute the fMRI-MEG fusion to acquire spatio-temporal data, we extract the lower

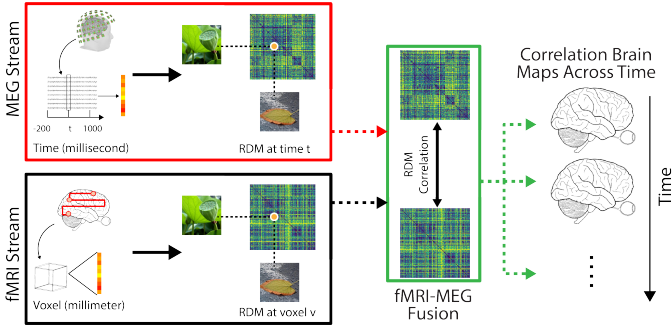


Fig. 4. fMRI-MEG Fusion. The red box shows the MEG stream of data. For MEG we have a time-series matrices of size [306, 1200] for each trial, we extract a vector of size $S = 306$ for all the sensors at each time point $T = 1200$. For fMRI stream (black box), we compute the RDMs by applying pre-defined masks of the same size as the data that capture the area for each region of interest. After extracting the activity patterns of the region of interest, we squeeze the 3D matrix to a 1D vector, resulting in a vector with varying size that is dependant on the total area of the voxel. In the green box, we compute the similarity (Spearman's correlation) between the fMRI RDMs at each voxel and MEG RDMs at each time point. Resulting in a 3D representational similarity correlations at each time point.

triangular of the RDMs and vectorize them for both fMRI and MEG. This is done to allow us to compute the similarity (Spearman's correlation) between the fMRI RDMs at each voxel and MEG RDMs at each time point (Figure 4). Given that each RDM is a symmetric square matrix, the lower triangular would hold the most meaningful representation. The fMRI/MEG fusion create a 3D representational similarity correlations at each time point, giving 3 dimensional view of neural activity in the brain.

D. T-Test Analysis

In this project, we utilize t-test analysis to investigate if there are significant difference between the distance reliability across twin sets. In this paper we run three t-tests, first we compare Mahalanobis distance with correlation, then Mahalanobis versus Euclidean is evaluated and lastly, correlation is compared with Euclidean. P-value threshold is considered 0.05 at the beginning and then it is updated using false discovery rate (FDR) multiple comparison correction method.

IV. RESULTS

Using the fMRI RDMs for twin set 1 and twin set 2, we computed the Pearson correlation coefficient of both twin set RDMs for each distance metric. This was done to determine the distance

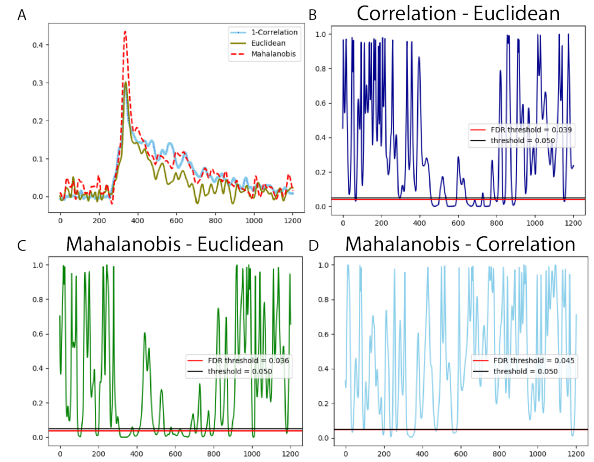


Fig. 5. MEG T-test Analysis. A. Shows the averaged correlation of twin set RDMs over all time points computed on all three distance metrics. B-D. Shows the t-test p-values over all time points of the correlated twin set RDMs. The black vertical line shows default threshold which is equal to 0.05 whereas red line is the FDR updated threshold.

metric that can reliably reproduce RDMs. Further, we performed paired t-test analysis to compare RDM similarity across three different distance metrics. Results from the t-test analysis shows that there no significant difference between Correlation, Euclidean, or Mahalanobis when computing RDMs for fMRI (Table I). It is also worth noting that the t-tests of IT brain region have overall lower p-values than that of Calcarine. Alternatively, table II shows the averaged computational time for fMRI and MEG RDMs on 50 iterations randomly generate data that consist of the dimensional size as the real fMRI and MEG data for each distance metric. That is, [306, 1200] for MEG and [53, 63, 52] for fMRI.

Figure 7A, shows the computed Pearson correlation coefficient of both twin set RDMs for each distance metric across all time points. Figure 7A suggest that Mahalanobis distance is the best metric to compute the RDMs for the MEG data, followed by Correlation then Euclidean distances. Figure 7B-D shows the results of computed t-test across all three distance metrics. These sets of figure and table III also show the time point at which each t-test comparison is significant.

Figure 6 the first row shows the the Spearman correlation (fusion) between MEG and fMRI RDM using all three distance metric in both brain regions (IT and Calcarine). In the IT region, the

TABLE I
FMRI TWIN SET T-TEST ANALYSIS

Distance Metrics	Brain Region	Results
Corr - Euclid	IT	$t(14) = .583, p = 0.569$
Corr - Maha	IT	$t(14) = -.598, p = 0.559$
Maha - Euclid	IT	$t(14) = .987, p = 0.340$
Corr - Euclid	Calcarine	$t(14) = -.011, p = 0.992$
Corr - Maha	Calcarine	$t(14) = .337, p = 0.741$
Maha - Euclid	Calcarine	$t(14) = -.246, p = 0.809$

TABLE II
RDM COMPUTATION TIME

Distance Metrics	Average RDM Computation Time
Correlation (Corr)	$M = 49.75s, SD = 20.50s$
Euclidean (Euclid)	$M = 45.26s, SD = 15.98s$
Mahalanobis (Maha)	$M = 178.87s, SD = 47.17s$

TABLE III
MEG TWIN SET T-TEST ANALYSIS
MINIMUM P-VALUE

Distance Metrics	Significant Time Period	Minimum P-value
Corr - Euclid	259ms	$p = 0.0391$
Corr - Maha	109ms	$p = 0.0359$
Maha - Euclid	333ms	$p = 0.0453$

Mahalanobis distance is the best metric to compute for fMRI/MEG based fusion, followed by Euclidean then Correlation distance. Alternatively for the Calcarine brain region, the Correlation distance is the best metric to compute for fMRI/MEG based fusion, followed by Mahalanobis then Euclidean distance. Figure 6 the second row shows the instance where t-test difference between distance measures is significant: (Mahalanobis – correlation), (Mahalanobis – Euclidean) and (Correlation – Euclidean) at each time point.

V. DISCUSSION

Our results suggests that the choice of distance metric to compute the RDM does not effect the reproducibility of the RDMs when dealing with fMRI data (Table I). This is particularly useful when considering that some distance metrics such as Mahalanobis distance take longer to compute(due to the use of the covariance matrix and its inverse; Table II). Euclidean distance being almost 4 times

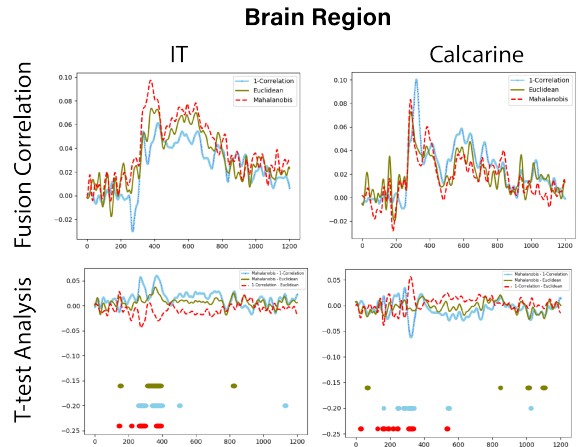


Fig. 6. fMRI/MEG Fusion Analysis. Figure (a) and (b) respectively represent the Spearman correlation between MEG and fMRI RDM for IT and calcarine locations. Figure (c) and (d) show the difference between distance measures: (Mahalanobis – correlation), (Mahalanobis – Euclidean) and (Correlation – Euclidean) and the time points each difference is significant based on hypothesis T-test for IT and calcarine respectively.

faster than Mahalanobis and 10% faster than correlation distance. As for the relatively lower p-values for IT in table I, this could be due to the fact that IT in the neuroscience literature is associated with object recognition. Considering the experimental task involve object recognition, it is likely that IT is capturing relatively more underlying information rather than noise compared to Calcarine. Hence, its effect is demonstrated in this analysis.

Alternately, when we evaluate the difference between distance measures in MEG RDMs between Twin Set 1 and 2 for all time points, we found that Mahalanobis distance is the best metric to compute the RDMs for the MEG data, followed by Correlation then Euclidean distances. Similarly with combined fMRI/MEG data, Mahalanobis distance is the most reliable metric to relate the RDMs of fMRI/MEG for IT resulting in the significantly highest correlation across twin sets.

A. Limitations

One major limitation is due to the computational cost being higher for fMRI, we were restricted to investigate only 2 brain regions. Alternatively, it would be more suitable to investigate all brain regions, as it could be the case that different brain regions perform better with different metrics.

REFERENCES

- [1] N. Kriegeskorte, M. Mur, and P. A. Bandettini, “Representational similarity analysis-connecting the branches of systems neuroscience,” *Frontiers in systems neuroscience*, vol. 2, p. 4, 2008.
- [2] A. Walther, H. Nili, N. Ejaz, A. Alink, N. Kriegeskorte, and J. Diedrichsen, “Reliability of dissimilarity measures for multi-voxel pattern analysis,” *Neuroimage*, vol. 137, pp. 188–200, 2016.
- [3] Y. Mohsenzadeh, C. Mullin, B. Lahner, R. M. Cichy, and A. Oliva, “Reliability and generalizability of similarity-based fusion of meg and fmri data in human ventral and dorsal visual streams,” *Vision*, vol. 3, no. 1, p. 8, 2019.
- [4] S. A. Huettel, A. W. Song, G. McCarthy *et al.*, *Functional magnetic resonance imaging*. Sinauer Associates Sunderland, MA, 2004, vol. 1.
- [5] R. A. Poldrack, J. A. Mumford, and T. E. Nichols, *Handbook of functional MRI data analysis*. Cambridge University Press, 2011.
- [6] M. X. Cohen, *Analyzing neural time series data: theory and practice*. MIT press, 2014.
- [7] H. Nili, C. Wingfield, A. Walther, L. Su, W. Marslen-Wilson, and N. Kriegeskorte, “A toolbox for representational similarity analysis,” *PLoS computational biology*, vol. 10, no. 4, p. e1003553, 2014.
- [8] N. Kriegeskorte and R. A. Kievit, “Representational geometry: integrating cognition, computation, and the brain,” *Trends in cognitive sciences*, vol. 17, no. 8, pp. 401–412, 2013.
- [9] M. Guggenmos, P. Sterzer, and R. M. Cichy, “Multivariate pattern analysis for meg: A comparison of dissimilarity measures,” *NeuroImage*, vol. 173, pp. 434–447, 2018.
- [10] R. M. Cichy, D. Pantazis, and A. Oliva, “Similarity-based fusion of meg and fmri reveals spatio-temporal dynamics in human cortex during visual object recognition,” *Cerebral Cortex*, vol. 26, no. 8, pp. 3563–3579, 2016.
- [11] R. M. Cichy and D. Pantazis, “Multivariate pattern analysis of meg and eeg: A comparison of representational structure in time and space,” *NeuroImage*, vol. 158, pp. 441–454, 2017.
- [12] S.-M. Khaligh-Razavi, R. M. Cichy, D. Pantazis, and A. Oliva, “Content-dependent fusion: Combining human meg and fmri data to reveal spatiotemporal dynamics of animacy and real-world object size,” in *2017 AAAI Spring Symposium Series*, 2017.
- [13] A. Khosla, A. S. Raju, A. Torralba, and A. Oliva, “Understanding and predicting image memorability at a large scale,” in *International Conference on Computer Vision (ICCV)*, 2015.
- [14] L. Chelazzi, E. K. Miller, J. Duncan, and R. Desimone, “A neural basis for visual search in inferior temporal cortex,” *Nature*, vol. 363, no. 6427, p. 345, 1993.

VI. APPENDIX

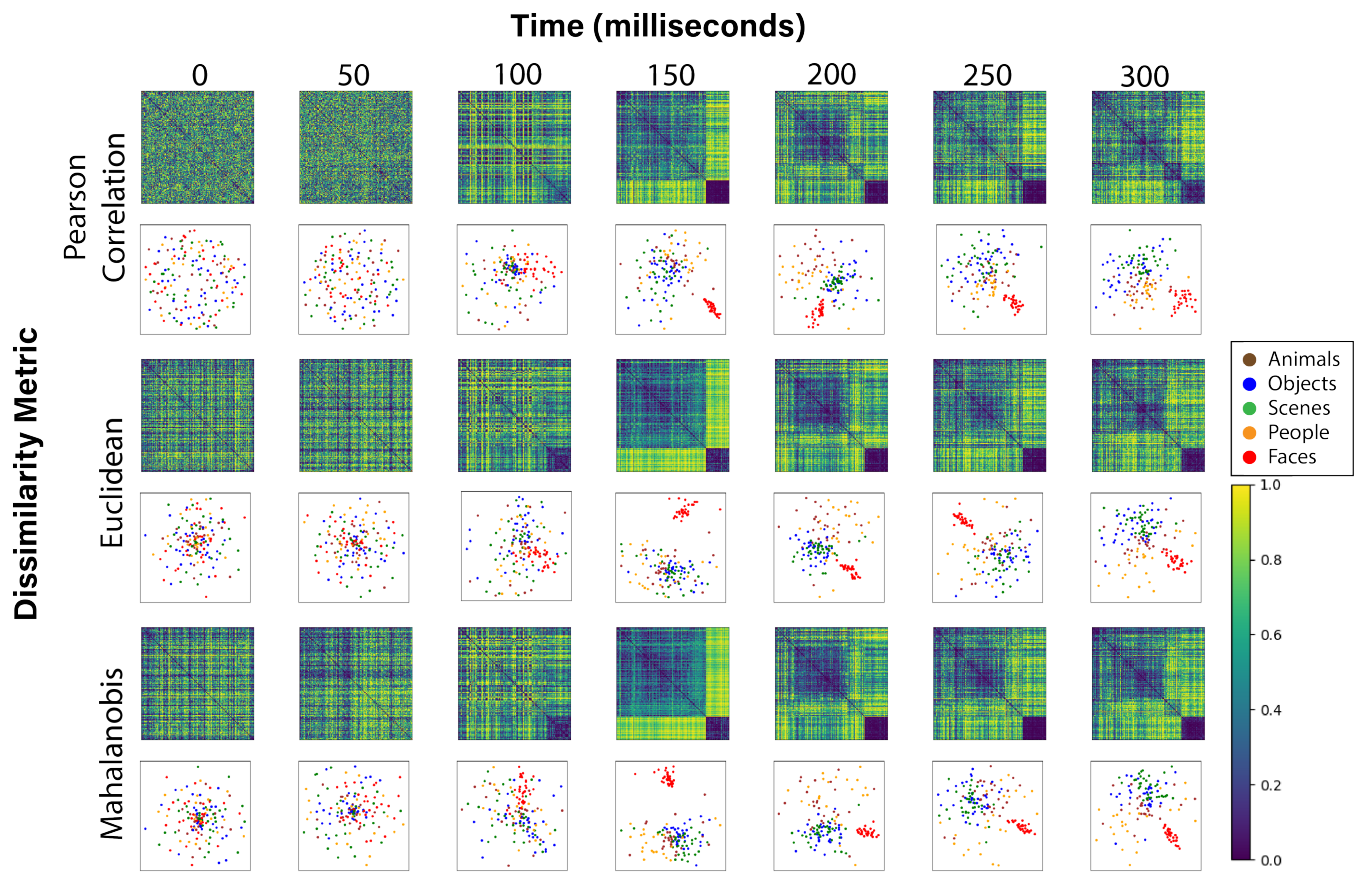


Fig. 7. MEG RDMs Across Time. Each pair of rows represents the RDM at specific time point and its subsequent Multidimensional scaling computed from each of the three metrics.

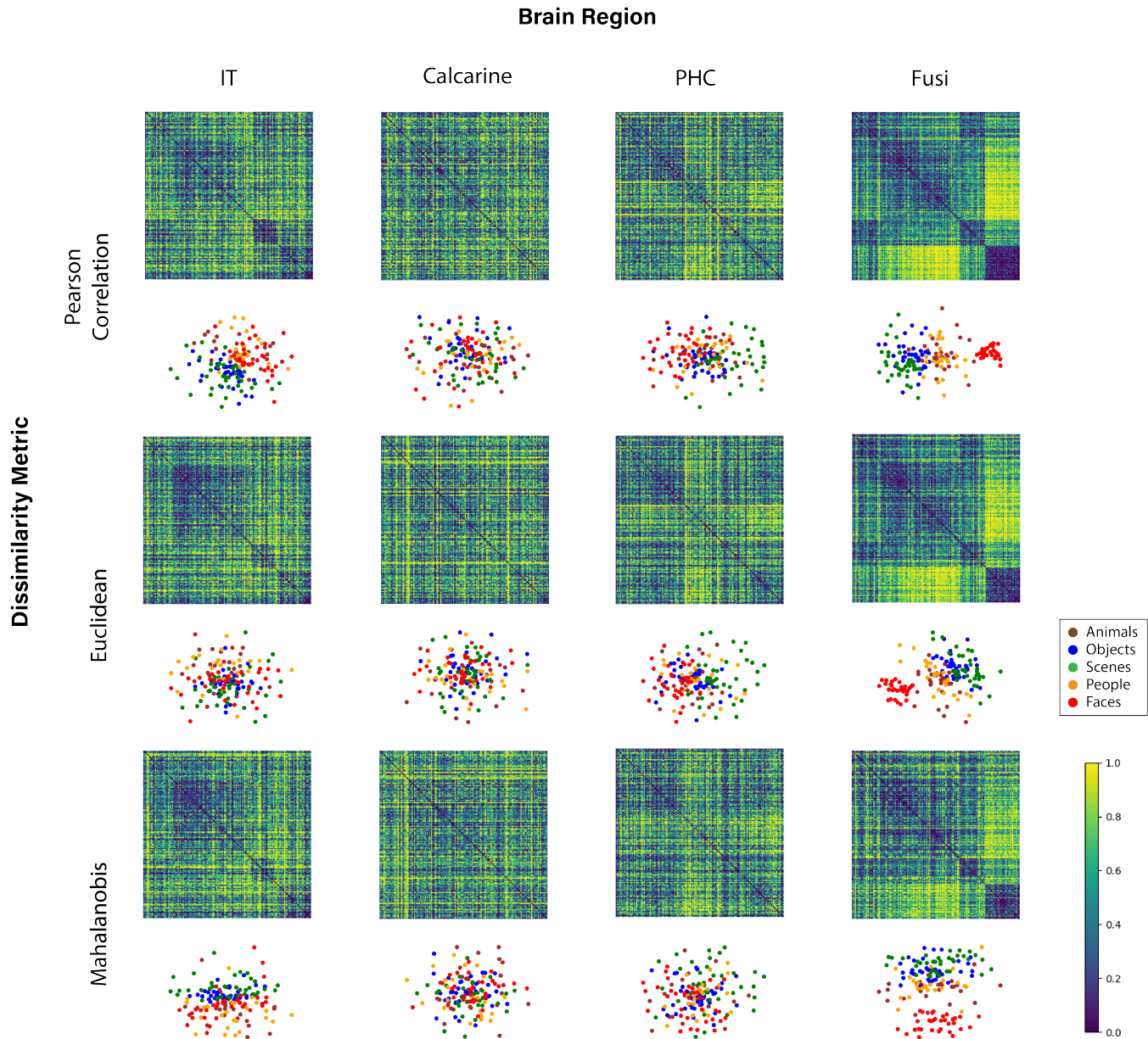


Fig. 8. fMRI RDMs Brain Regions. Each pair of rows represents the RDM at specific brain region and its subsequent Multidimensional scaling computed from each of the three metrics.